

SQUIDS- *Superconducting Quantum Interference Devices*

G. Aviv¹

¹Department of Physics, Ben-Gurion University of the Negev, P.O. Box 653, Be'er-Sheva 84105, Israel.

Experimental physics course (2008)

Submitted to: Prof. Jung Grzegorz

(Dated: May 10, 2008)

The SQUID, "Superconducting Quantum Interference Device", was first built in the sixties. Since then numerous scientists have been working and developing this incredible device. In this paper I will try to give a glimpse of this wonderful world of superconducting devices. This paper is mainly based on two books (Barone Antonio and Gianfreanco Paterno (1982))[7] and (T. Van Duzer and C. W. Turner (1999))[6] and a few papers. First I will give a brief explanation of the basic aspects of superconductivity regarding SQUIDs, such as Meissner effect, Cooper pair tunneling and Josephson junction. Further, We will discuss one junction and multi junction SQUIDs. And last but not least SQUID magnetometers.

I. THEORY

A. The Meissner effect

The Meissner experiment was a milestone in the history of superconduction, done by Meissner and Ochsenfeld[5] in 1933. They had been working on perfectly pure crystals of a normal metal in which resistance vanishes at $T = 0$ because of the elimination of phonon scattering. In this experiment they compared the behavior of this kind of metal to superconductors.

In this section we will examine the behavior of a conductor subject to an ac field. In an electron gas with an applied electric field \vec{E} , there are two opposing influences on the momenta of the electrons. Therefore the differential equation for the average x -directed electron velocity can be written as

$$m \frac{d\langle v_x \rangle}{dt} + \frac{m\langle v_x \rangle}{\tau} \quad (1)$$

where τ is the momentum of relaxation time and e is the magnitude of the electronic charge. If we let $d\langle v_x \rangle/dt \cong \partial\langle v_x \rangle/\partial t$ in equation 1 we obtain

$$\langle v_x \rangle = \frac{(-e\tau/m)E_x}{1 + j\omega\tau} \quad (2)$$

The expression for the ac current density is:

$$J_x = \frac{ne^2\tau/m}{1 + \omega^2\tau^2}(1 - j\omega\tau)E_x \quad (3)$$

Now we should inspect the results while letting the relaxation time τ to become infinite:

$$J_x = -j(ne^2/\omega m)E_x \quad (4)$$

And after further derivation (T. Van Duzer ch.1)[6]:

$$\frac{\partial^2 \dot{B}_z}{\partial y^2} = \frac{\mu_0 ne^2}{m} \dot{B}_z \quad (5)$$

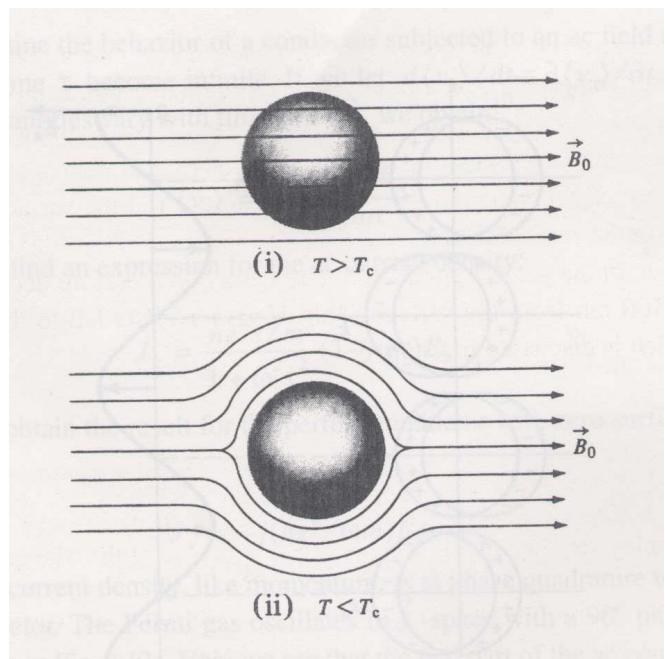


FIG. 1: Superconductor sample subjected to an applied magnetic field with temperature (i) above and (ii) below T_c . The flux expulsion below T_c is called Meissner effect[6]

The general solution of 5 can be written in the form:

$$\dot{B}_z = A_1 e^{\alpha y} + A_2 e^{-\alpha y} \quad (6)$$

Where $\alpha = (\mu_0 ne^2/m)^{1/2}$. The solution that meets the boundary condition at infinity is one in which \dot{B}_z decay exponentially with distance from the boundary. Where the $1/e$ distance of decay is typically less than 100 nm. Therefore we see that under these conditions no weak magnetic field will penetrate to the interior of a perfect conductor.

B. Cooper Pair Tunneling

In this section we introduce the concept of tunneling of Cooper pairs. Pair tunneling doesn't involve excitation and can occur even without bias across the junction, there is minimum current under no voltage would be developed if current were carried across the insulator by Cooper pairs.

Cooper pairs tunneling through the barrier constitute a supercurrent

$$I = I_0 \sin \delta \quad (7)$$

Where I_0 is the critical current and δ is the difference between the phases of the order parameters in the two superconductors. In case of zero applied current [3], the two electrodes are coupled by an energy $I_0 \Phi_0 / 2\pi$. In the absence of thermal fluctuations, the voltage V across the barrier is zero for $I < I_0$; for $I > I_0$ a voltage is developed and δ evolves with time as

$$\dot{\delta} = 2eV/\hbar = 2\pi V/\Phi_0 \quad (8)$$

For low- T_c junctions, the current-voltage characteristics are well explained by the resistivity and capacitively shunted junction (RCSJ) model. [4] In this model, The Josephson element is in parallel with resistance R and capacitance C . In the case of SQUIDS, one generally needs nonhysteretic $I - V$ characteristics, a requirement that is met if

$$\beta_c \equiv 2\pi I_0 R^2 C / \Phi_0 \lesssim 1 \quad (9)$$

In the limit $\beta_c \ll 1$ which is often the case for high T_c junctions, the RCSJ model is reduced to the RSJ model and the $I - V$ characteristic is given by $V = R(I^2 - I_0^2)^{1/2}$ for $I \geq I_0$.

C. Josephson Junctions

The Josephson junction [2] is a junction between two superconductors which are weakly coupled separated (in the case of low- T_c Tunnel junction) by thin insulating barrier. Under this condition, cooper pairs of electrons can pass from one superconductor to the other even with no applied voltage. There are numerous ways to perform Josephson junctions both for metallic [low-temperature superconductors (LTS)] and oxide [high-temperature superconductors (HTS)]. These including metal or semiconductor links, grain boundaries, very narrow constrictions, damaged regions, and, most prominently, insulating tunnel barriers. Tunnel junctions play important roll in LTS electronics. Therefore tunnel junction is in use in many Josephson junctions.

In 1962 B. D. Josephson [2] suggested that electron pair could tunnel between closely spaced superconductors even with no potential difference. Anderson and Rowell [3] observed this effect in 1964.

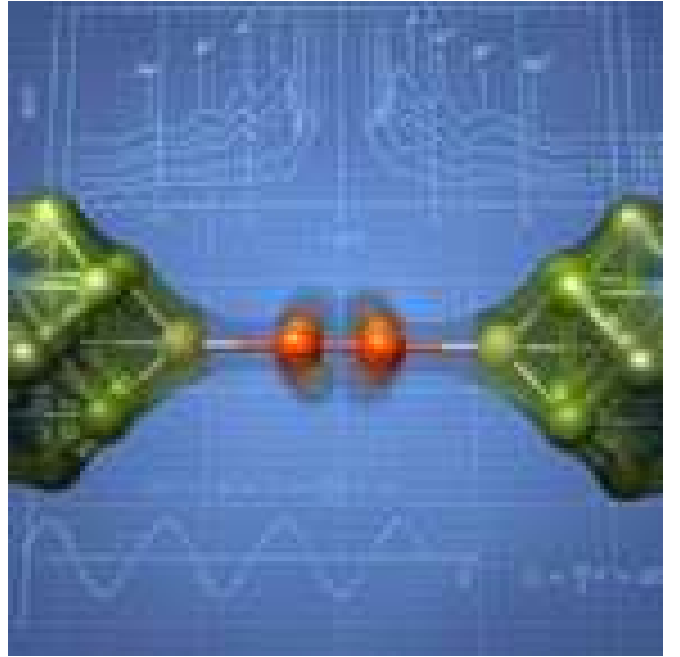


FIG. 2: Josephson Junctions, first applied by, John Rowell and Philip Anderson at Bell Labs (1963).

This effect explained by simple derivation of the Josephson relations, The pair tunneling current seems to depend on the difference of phase of effective wave functions across the barrier.

This discovery opened the physics world the ability to create devices such as SQUID and to set the Josephson voltage standard. [6]

II. SQUIDS: THEORY AND APPLICATIONS

The configuration we describe in this section is class of devices known as SQUIDS: "*Superconducting Quantum Interference Devices*". The SQUIDS are superconducting devices who measure magnetic flux and output voltage signal, which is periodic function of a flux threading a superconducting loop in which one or two weak links are inserted. The maximum flux variation SQUIDS can measure is in the order of $\sim 10^{-5} \Phi_0$ [14] where $\Phi_0 = 2.07 \times 10^{-15}$ weber.

The single junction SQUIDS also known as RF-SQUIDS the junction is shorted by superconductor path; therefore the voltage response obtain by coupling the loop to a RF bias tank circuit.

The double junction SQUIDS also known as DC-SQUIDS. In this device the two weak links are not shorted by superconductor path; therefore the DC current-voltage characteristics can be observed. This device applies current who slightly greater then the critical current and one can monitor the voltage drop across the device.

In this chapter we will observe the basic principles of

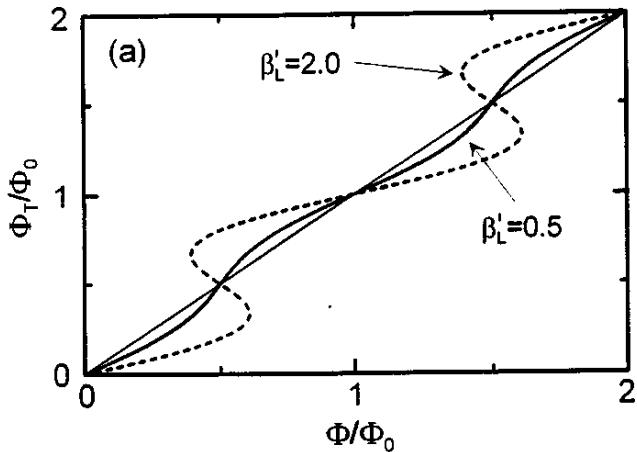


FIG. 3: The rf SQUID: (a) Normalized total flux Φ_T/Φ_0 vs normalized applied flux Φ/Φ_0 for $\beta'_L = 0.5$ [14]

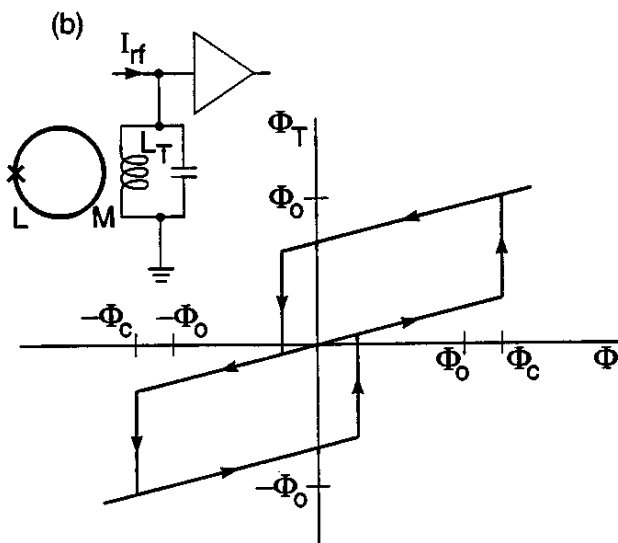


FIG. 4: The rf SQUID: (b) Total flux Φ_T vs applied flux Φ for rf SQUID with $LI_0/\Phi_0 = \frac{5}{4}$, showing transitions between quantum states in absence of thermal noise as Φ is increased and subsequently decreased. Inset shows rf SQUID inductively coupled to the inductor of a resonant circuit.[14]

operation, maximum sensitivity and practical measurement technics.

A. One-Junction SQUIDS

The rf SQUID [8][9][10] (1970) consists of a single Josephson junction integrated into a superconducting loop that is inductively coupled to the inductance L_T of an LC tank circuit. [inset Fig. 4]. The tank circuit is driven by an rf current, and the resultant rf voltage is periodic in the flux applied to the SQUID with period Φ_0 .

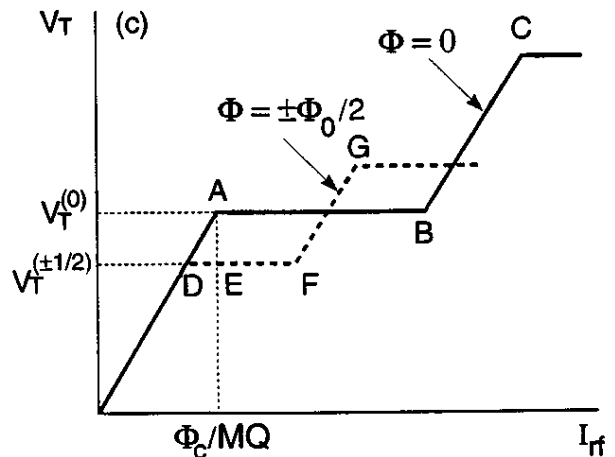


FIG. 5: The rf SQUID: (c) Peak rf voltage V_T across tank circuit vs peak rf current I_{rf} in absence of thermal noise for $\Phi = 0$ (solid line) and $\Phi = \pm\Phi_0/2$ (dashed line).[14]

First we should check the total flux in the SQUID:

$$\Phi_T = \Phi - LI_0 \sin(2\pi\Phi_T/\Phi_0) \quad (10)$$

One can notice that Eq. 10 can exhibit two distinct kinds of behavior [inset Fig. 3]. For $\beta'_L = 2\pi LI_0/\Phi_0 < 1$, the slope is:

$$\frac{d\Phi_T}{d\Phi} = [1 + \beta'_L \cos(2\pi\Phi_T/\Phi_0)]^{-1} \quad (11)$$

One can see that for $\beta'_L < 1$ Eq.11 is always positive and Φ_T vs Φ curve is nonhysteretic. Alternately for the case of $\beta'_L > 1$, there is a region which Eq.11 is positive, negative or divergent so the Φ_T vs Φ curve become hysteretic. RF SQUIDS have been operated in both mods. While working in hysteretic mode the SQUID makes transition between quantum states and dissipates energy at a rate that is periodic in Φ . This periodic dissipation in turn modulates the quality factor Q of the tank circuit, so that when it is driven on resonance with a current of constant amplitude the rf voltage is periodic in Φ . On the other hand while $\beta'_L < 1$ the SQUID behaves as a parametric inductance, modulating the effective inductance and hence the resonant frequency of the tank circuit as the flux is varied. Thus when the tank circuit is driven at constant frequency, the variations in its resonant frequency cause the rf voltage to be periodic in Φ . Historically, most of the low- T_C rf SQUIDS were operated in the hysteretic mode, although there are advantages to the nonhysteretic mode.

If we consider the one junction SQUID as a circuit element Fig.7 the current through the inductor is [6]:

$$I_L = I - I_C \sin(\beta_L \frac{I_L}{I_C}) \quad (12)$$

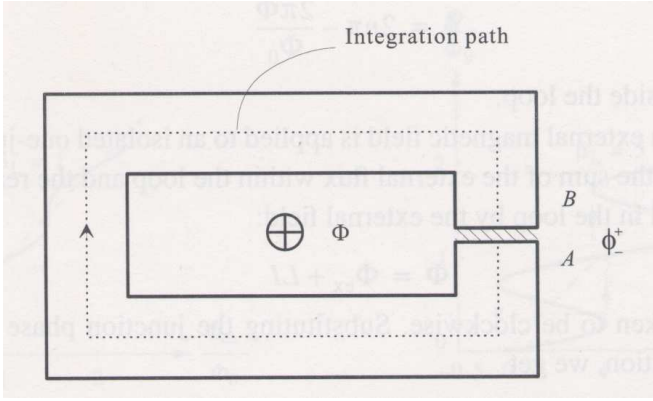


FIG. 6: Two-junction parallel array with symmetrical feed. The integration path for the analysis is shown by the broken line.[6]

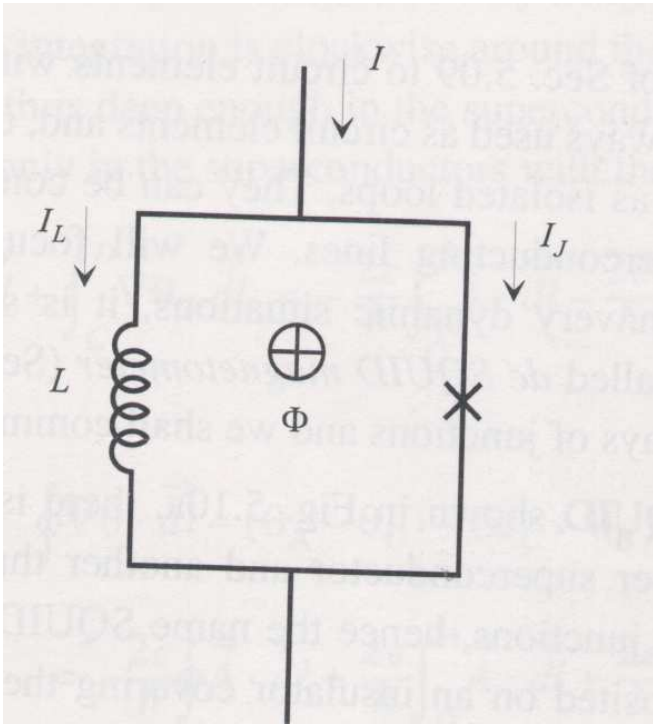


FIG. 7: Equivalent circuit of a one-junction SQUID.[6]

B. Multi-Junction SQUIDs

These SQUIDs are made with more than one junction and always be used as circular elements, unlike the rf-SQUIDs they are not found in application as isolated loops. The two Josephson junction SQUIDs are called *dc-SQUIDs*[13] (1964). The junctions are connected in parallel on a superconducting loop of inductance L [inset Fig.9(a)]. In this type of SQUID we should apply constant bias current $I_B > 2I_0$ the voltage V across the SQUID oscillates with period Φ_0 as one changes the external magnetic flux Φ [inset Fig.9(b,c)].

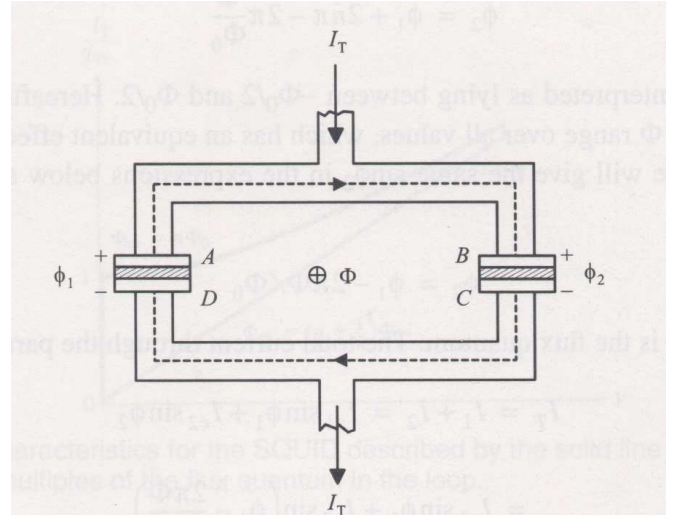


FIG. 8: Two-junction parallel array with symmetric feed.[6]

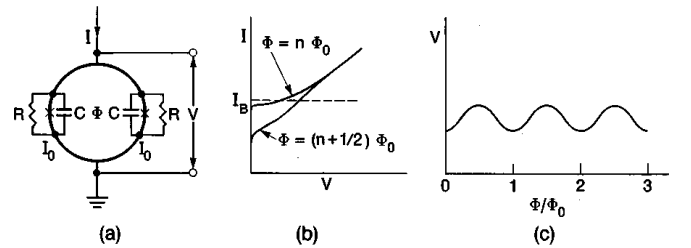


FIG. 9: The dc SQUID: (a) schematic, (b) $I-V$ characteristic, (c) V vs Φ/Φ_0 at constant bias current I_B . [14]

In the dc SQUID as in Fig.8, there is a common electron-pair wave function throughout the upper superconductor and another throughout the lower one. These wave functions weakly interfere throughout the junction. If magnetic flux is passed through the loop, it changes the relation between the phase difference across the two junctions. As a result the critical current of the SQUID is changed.

To measure small changes in Φ ($\ll \Phi_0$) it is better to choose the bias current to maximize the amplitude of the voltage modulation and sets the external flux at $(2n+1)\Phi_0/4$ ($n = 0, 1, 2, \dots$), so that the flux-to-voltage transfer coefficient $|\partial V/\partial \Phi|$ is maximized, which we denote as V_Φ . In this way the SQUID will produce a maximum output voltage signal $\delta V = V_\Phi \delta \Phi$ in response to a small flux signal $\delta \Phi$.

Let's find the relationship between δ_1 and δ_2 for the dc SQUID while Φ is the flux in the loop:[6]

$$\delta_2 = \delta_1 - 2\pi \frac{\Phi}{\Phi_0} \quad (13)$$

where $\Phi_0 = h/2e$, is the flux quantum. Now we shall see the total current through the parallel junction is:

$$I_T = I_1 + I_2 = I_{c1} \sin \delta_1 + I_{c2} \sin \delta_2$$

$$= I_{c1} \sin \delta_1 + I_{c2} \sin(\delta_1 - \frac{2\pi\Phi}{\Phi_0}) \quad (14)$$

where the critical currents I_{c1} and I_{c2} of the two junctions are assumed to be generally unequal.

If we will neglect the self induced flux we donate Φ in 13 as Φ_{ex} and treat it as independent parameter. The maximum zero-voltage current is found by maximizing 14 with respect to δ_1 ; the result is:

$$I_{Tc}(\Phi_{ex}) = [(I_{c1} - I_{c2})^2 + 4I_{c1}I_{c2} \cos^2(\pi\Phi_{ex}/\Phi_0)]^{1/2} \quad (15)$$

now if we take $I_{c1} = I_{c2}$ Ex.15 become:

$$I_{Tc}(\Phi_{ex}) = 2I_{c1} \left| \cos \frac{\pi\Phi_{ex}}{\Phi_0} \right| \quad (16)$$

To consider how the magnetic field affects the $I-V$ characteristic of a typical junction pair for nonhysteretic junction Fig.11 for a whole number of flux quanta or half flux quanta.

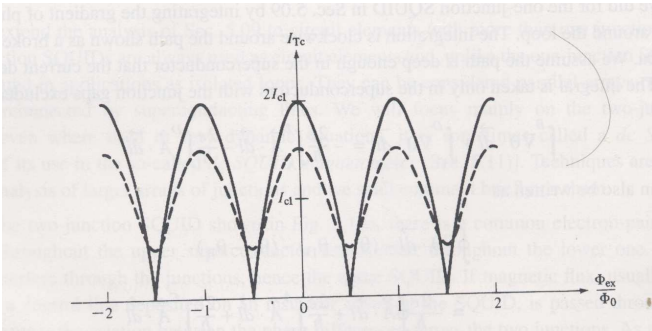


FIG. 10: Dependence of the critical current of two-junction SQUID on the applied flux where the self induced flux is neglect. Solid lines for symmetrical SQUIDs ($I_{c1} = I_{c2}$) and broken line for asymmetrical SQUID with $I_{c1} = 2I_{c2}$. If the meaning of Φ (here $\Phi = \Phi_{ex}$) in (3) were retained, the periodic succession of lobes seen here would be represent by $n = -2, -1, 0, 1, 2$. [6]

III. SQUID MAGNETOMETERS

SQUIDs are highly sensitive devices for measuring magnetic flux. Their sensitivity level is high as it allows them to measure magnetic field from the human hearts and brains with high accuracy. here we will discuss several technics in which rf and dc SQUIDs been use for measuring magnetic fields and the advantages and drawbacks of each of the technics.

A. dc SQUID Magnetometers

The dc SQUID detection method depends on modulation of the position of the overall $I-V$ characteristic.

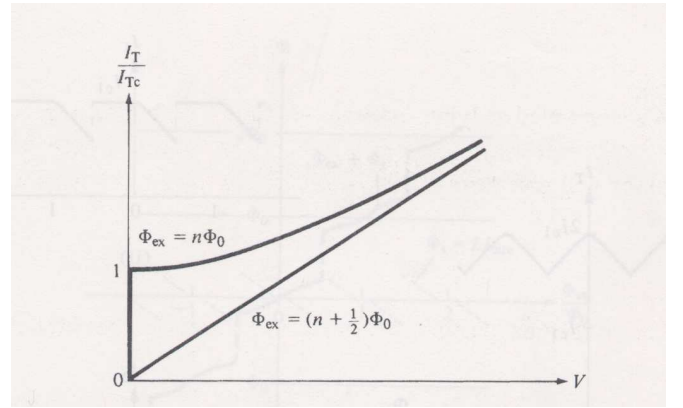


FIG. 11: $I-V$ characteristics for the SQUID described by the solid line, for integer and half-integer multiples of the flux quantum in the loop. [6]

The $I-V$ characteristic of the junction should be nonhysteretic therefore $\beta'_L < 1$. As we saw in II B the total critical current I_{Tc} is modulated by an applied external magnetic flux and has repetitive variation with period Φ_0 . The amount of modulation of I_{Tc} for the pair depends on the inductance L of the loop and the critical current of the junction, as seen in 12. From numerical calculation show that the optimal design has $LI_c/\Phi_0 \approx 0.5$ [6].

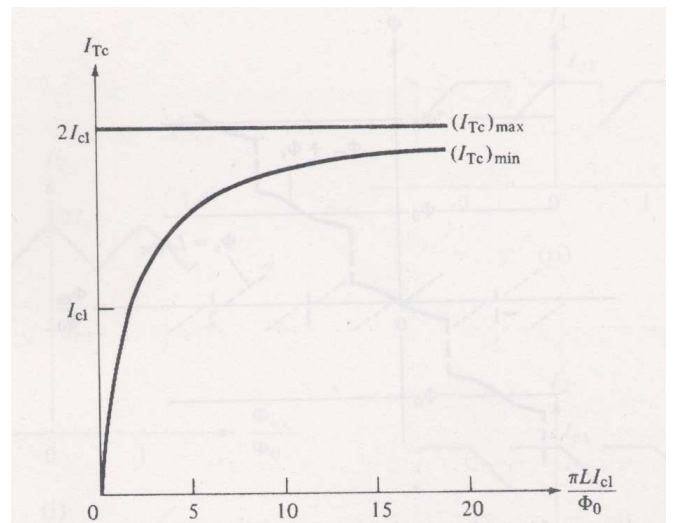


FIG. 12: Dependence of the maximum and minimum values of the total critical current on the loop inductance and single-junction critical current. The difference between these curves measures the modulation of I_{Tc} achieved with an applied magnetic field. [6]

As the external magnetic flux is changed and I_{Tc} thereby is modulated, the SQUID response is creation of voltage modulation along itself. This voltage modulation is similar for dynamic resistance R_D times the modulation of the critical current, $\Delta V \approx R_D \Delta I_{Tc}$ as seen in Fig.13. While modulating I_{Tc} the shape of $I-V$ characteristic, as a result of circulating currents following

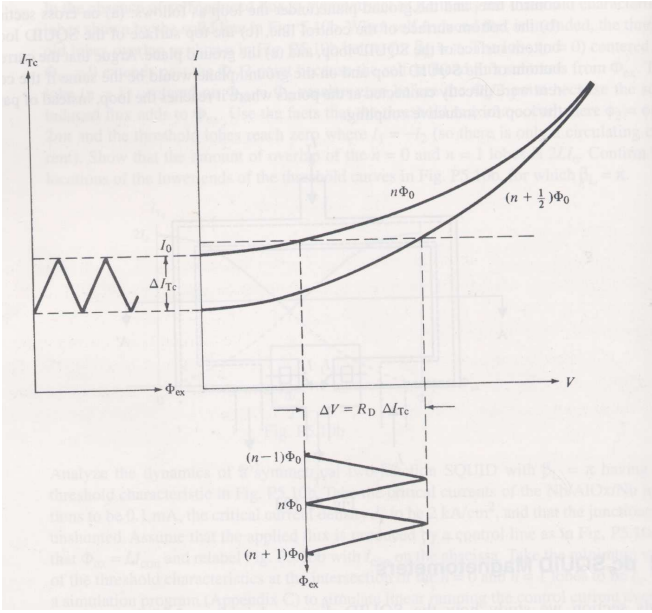


FIG. 13: Voltage variation across the dc SQUID resulting from modulation of the maximum zero-voltage current by an externally applied flux through the SQUID loop. I_{Tc} varies with Φ_{ex} ; its values with $n\Phi_0$ is designated I_0 . [6]

the Josephson frequency [6] and its harmonics. We wish to reach the possible maximum ΔV so it is required to set the current bias so average voltage satisfies:

$$V < \frac{2\Phi_0 R_D}{\pi L} \quad (17)$$

for all Φ_{ex} .

For finding the resolution of the SQUID [15] one should look at its equivalent flux noise $\Phi(f)$, which has spectral density $S_{V(f)}/|\partial V/\partial \Phi|$ where $S_{V(f)}$ is the spectral density of the voltage noise at a given current bias. [16][20]

There are two constraints that are imposed on the SQUID by thermal noise. One, the Josephson coupling energy [6] of each junction must be much greater than $K_B T$. The second constraint is on inductance. In SQUID the numerical analysis indicated that

$$L < \frac{\Phi_0^2}{5k_B T} \quad (18)$$

from which we can calculate that $L < 15\text{nH}$ at $T = 4.2\text{K}$. and the flux noise energy is [6]

$$\epsilon(f) \cong 16K_B T \left(\frac{LC}{\beta'_L}\right)^{1/2}, \quad \beta'_L < 1 \quad (19)$$

From here it's easy to see that by reducing T , L and C the resolution improves.

Flux Transformers:

In this device the magnetic flux is coupled to the low inductance SQUID loop from a larger external pick-up loop. The small loop couples the SQUID and they are shielded

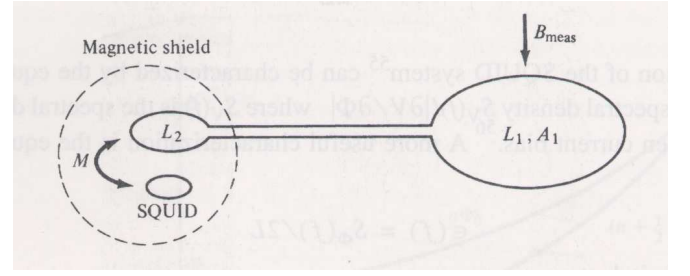


FIG. 14: Transformer used to enhance the sensitivity of a SQUID. the SQUID loop may contain one or two junctions for the use in RF or dc systems.

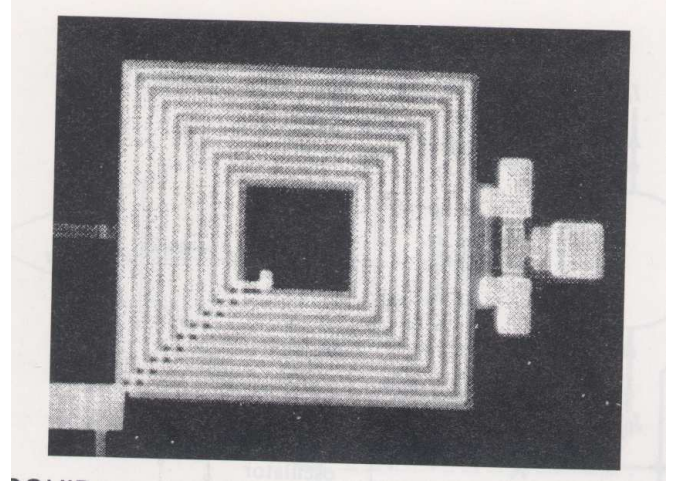


FIG. 15: Planar SQUID transformer with multi turn spiral primary. [6][17]

from external magnetic fields. When a magnetic field B_{mean} is applied to the large loop of area A_1 , a current I flows in the loop as needed to keep the flux inside the superconducting transformer at its original value. From here we can see that:

$$(L_1 + L_2)I = B_{mean}A_1 \quad (20)$$

The flux coupled into the SQUID loop from L_2 can be expressed by the mutual inductance term M between them ($\Phi = MI$). Due to the fact that the current is similar in both loops

$$\Phi = \frac{MB_{meas}A_1}{L_1 + L_2} \quad (21)$$

By adjusting the parameters a factor of ten in the sensitivity can be achieved [6]. An important achievement in sensitivity was made by using multi turn coils as in Fig. 16 [17]. The mutual inductance is enhanced in proportion to the number of turns.

Gradiometer:

In this device the transformer arrangement is modified as in Fig. 16. Where the two coils, called L_1 and L_2 , have opposite senses, therefore this device is measuring the

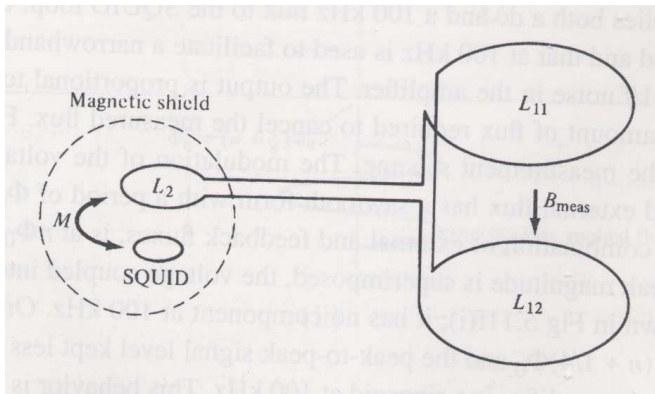


FIG. 16: Gradiometer arrangement of flux transformers. Currents induced in L_{11} and L_{12} cancel each other if B_{beam_s} is a uniform field.[6]

gradient of the magnetic field rather than the field itself. By using this technic one can almost eliminate far magnetic fields because their gradient is much smaller the very low power nearby sources. This device is been use, for example, to measure magnetic fields in the human body.

Read-Out electronics:

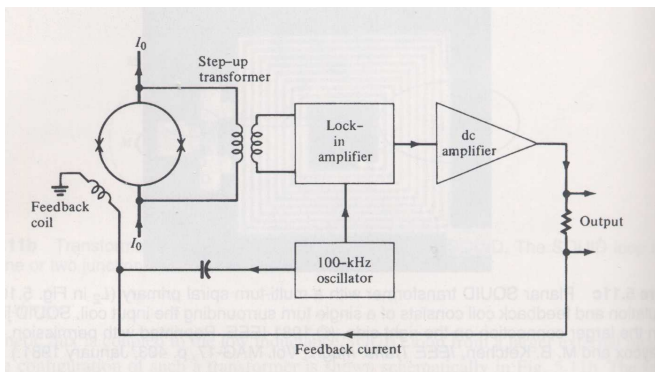


FIG. 17: Simple diagram of the circuit use to measure the voltage across the SQUID loop.[6]

The basic configuration for the read-out electronics from dc SQUID can be seen in Fig.17 The left side coil applies both DC and 100kHz flux to the SQUID loop. The prepuce of the DC flux is to cancel the flux been measured and the 100kHz used to facilitate a narrow band, the peropus of the lock in amplifier is to cancel the $1/f$ noise in the amplifier. The output is proportional to the feed back current, means the amount of current required to cancel the the measured flux.

B. rf SQUID Magnetometers

On the early days of the SQUID the commercial ones where of the RF type; Although its sensitivity is generally lower then the dc type SQUIDS [6]. The discovery

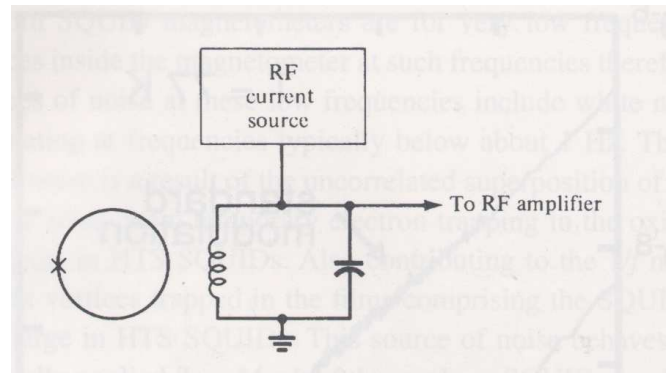


FIG. 18: Basic circuit of the RF SQUID

of the high-temperature oxide superconductors reinvigorated interest in the RF SQUIDS. The advantages of the RF SQUID came from its simplicity (one junction), improving HTS materials and read out electronics that raised it frequency.

As mentioned in II A a loop with one Josephson junction, is coupled to a turn circuit driven by an RF source and the quasistatic applied flux is changed, there is a periodic variation of the loading on the tank circuit and, therefore, of the RF voltage across the tank circuit, by the SQUID loop as a function of applied flux. A feedback loop is been used and is based on periodic dependence of a SQUID property on applied flux.

The operating can be understood in terms of the solution of the quasistatic relation [6]

$$\Phi_1 = \Phi_{ex} - LI_c \sin \frac{2\pi\Phi_1}{\Phi_0} \quad (22)$$

Where Φ_1 is the flux inside the loop..

As mentioned in section II A The RF SQUID has two operation modes *hysteretic* and *nonhysteretic* modes. In the *hysteretic* mode the negative portions of the curve are unstable. thus, as the external flux varied the internal flux follows a path only along portions of the curve with positive slopes.

In the *nonhysteretic* or *inductive* mode, the diversions from a diagonal strait line are smaller and there are no portions of the curve with negative slope.

In the hysteretic mode the operation depends on the periodic dependence of the loss in the SQUID loop in the magnitude of the applied quasistatic magnetic field. As seen in Fig. 19 the locus of of points traced out on the $\Phi_1 - \Phi_{ex}$ curve for an assume magnitude of RF applied flux Φ_{RF} . In the usual method of operation, the RF current in the coil which applies flux is set to a large enough value that the SQUID loop is driven around hysteretic and loosely path on the $\Phi_1 - \Phi_{ex}$ curve. But, once the lossy transition is made, the oscillation level in the turn circuit decrees and it grows to another transition. The oscillation amplitude is kept at the right value to cause transitions, and the amplitude depends on the periodically on the quasistatic applied flux, as illustrated in Fig.

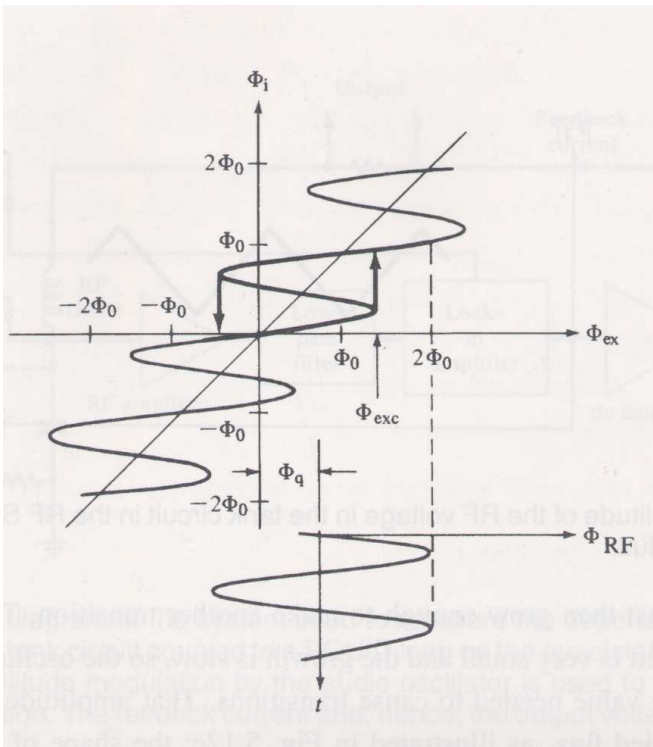


FIG. 19: Relation between the flux inside the SQUID loop and the external flux in the loop area for $LI_c/\Phi_0 > 1/2\pi$. With sufficient applied RF flux, a lossy hysteretic path is followed. The quasistatic flux applied to the loop causes an offset and leads to switching at Φ_{exc} with lower level of RF flux.[6]

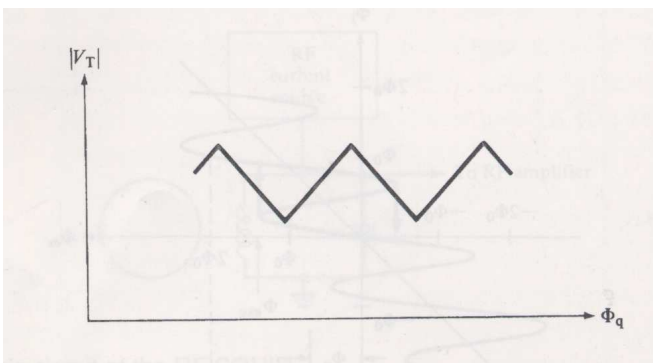


FIG. 20: Amplitude of the RF voltage in the tank circuit in the RF SQUID as function of the applied quasistatic flux.[6]

20 the triangle shape by adjusting the coupling between the tuned circuit and the SQUID loop.

The other mode of operation is the nonhysteretic occurs when $\Phi_1 - \Phi_{ex}$ relation is single-valued.[18] In this case the Josephson junction remains in the same zero-voltage state and there are no crucial loss in the SQUID loop. But, there is periodic variation of the SQUID loop reactive loading in the tuned circuit as the applied quasistatic flux Φ_q through the SQUID loop is varied linearly. The SQUID loop current, through the mutual in-

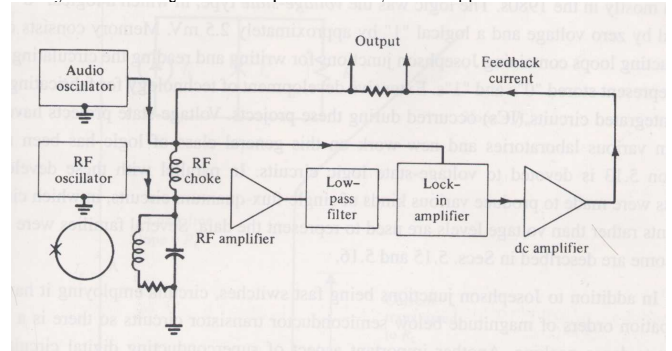


FIG. 21: Simplified diagram of the system used to measure the dependence of the magnitude of the RF voltage in a tank circuit coupled to a SQUID loop on the quasistatic applied magnetic flux to be measured.[6]

ductance, produces a reaction on the RF tuned circuit and effect its voltage.[6]

The read-out electronics for both modes shown in Fig. 21. A $\sim 10\text{kHz}$ low frequency modulation is used same as for the dc SQUIDS magnetometer. In the past the RF was in the order of $10 - 30\text{MHz}$. In the last two decades the SQUID system have included the use of thin film planer resonator and SQUID loops and the use of MW frequency. The higher frequency lowered the white noise. Now days a great effort devotes for the use of HTS materials with operation in 77K .[19] The ability to use HTS and low scale lithography makes SQUIDS cheaper smaller and with much larger scale of use. The ability to miniature the SQUIDS to the micro scale allows the creation of high sensitive brain imaging machines based on hundreds of SQUIDS (such as in Bob Kraus SQUID team at Los Alamos).

Acknowledgments

I wish to thank Prof. J. Grzegorz for introducing me to this most interesting field in physics.

-
- [1] J. M. Ziman, *Electrons and Phonons*, Oxford: Oxford University Press, 1960.
 [2] B.D. Josephson, *Phys. Lett.*, Vol. 1 pp. 251-253, 1962.
 [3] P.W. Anderson and J.M Rowell, *Phys.Rev. Lett.*, Vol. 10 pp. 230-232, 1963.

- [4] McCumber, D. E Stewart, *J. Appl. Phys.*, **39**, 3113, 1968.
 [5] W. Meissne and R. Ochsenfeld, *Naturwissenschaften*, Vol. 21 pp. 787-788, 1933.
 [6] T. Van Duzer and C. W. Turner, *Superconductive devices and Circuits Prentice Hall PTR, QC611.92V36 2nd ed.*

- 1998.
- [7] A. Barone and G. Paterno, *Physics and Applications of the Josephson Effect New York: Wiley, 1982*, QC176.8T8B37 1982.
- [8] Mercereau, J. E., *Rev. Phys. Appl.*, **5**, 13 1970.
- [9] Nisenoff, M., *Rev. Phys. Appl.*, **5**, 21 1970.
- [10] Zimmerman, J. E., P. Thiene, and J. T. Harding, *J. Appl. Phys.*, **41**, 1572 1970.
- [11] Jackel, L. D., and R. A. Buhrman, *J. Low Temp. Phys.*, **19**, 201. 1975.
- [12] Ehnholm, G. J., *J. Low Temp. Phys.*, **29**, 1. 1977.
- [13] Jaklevic, R. C., J. Lambe, A. H. Silver, and J. E. Mercereau, *Phys. Rev. Lett.*, **12**, 159. 1964.
- [14] D. Koelle et al., *Reviews of Modern Physics*, Vol. **71**, No. 3, 1999
- [15] J. Clarke, W. M. Goubau, and M.B. Ketchen, *J. Low Temp. Phys.*, Vol. 2,pp. 99-144 1976.
- [16] J. Clarke, *Proc. IEEE*, Vol. 77,pp. 1208-1223 1989.
- [17] J. M. Jaycox and M. B. Ketchen, *IEEE trans. Magn.*, Vol. MAG-17,pp. 400-403 1981.
- [18] S. N. Erne and H. D. Hahlbohm, and H. Lubbig, *J. Appl. Phys.*, Vol. 47,pp. 5440-5442 1976.
- [19] B. Chesca, *J. Low Temp. Phys.*, Vol. 110,pp. 963-1001 1998.
- [20] Tesche, C. D., and J. Clarke,, *J. Low Temp. Phys.*, **29**, 301. 1977.